Human Molecular Genetics, 2012, Vol. 21, No. 4 ***874–889***
doi:10.1093/hmg/ddr521
Advance Access published on November 10, 2011

Selective neuroprotective effects of the S18Y polymorphic variant of UCH-L1 in the dopaminergic system

Maria Xilouri[1,*], Elli Kyratzi[1], Pothitos M. Pitychoutis[2], Zoi Papadopoulou-Daifoti[2], Celine Perier[3], Miquel Vila[3,4,5], Matina Maniati[1], Ayse Ulusoy[6,†], Deniz Kirik[6], David S. Park[7], Keiji Wada[8] and Leonidas Stefanis[1,9,*]

[1]Division of Basic Neurosciences, Biomedical Research Foundation of the Academy of Athens, Athens, Greece, [2]Department of Pharmacology, Medical School, University of Athens, Athens, Greece, [3]Neurodegenerative Diseases Research Group, Vall d'Hebron Research Institute-Center for Networked Biomedical Research on Neurodegenerative Diseases (CIBERNED), Barcelona 08035, Spain, [4]Catalan Institution for Research and Advanced Studies (ICREA), 08010 Barcelona, Spain, [5]Department of Biochemistry and Molecular Biology, Autonomous University of Barcelona, 08193 Bellaterra, Barcelona, Spain, [6]Brain Repair and Imaging in Neural Systems, Department of Experimental Medical Science, Lund University, Lund, Sweden, [7]Neuroscience Lab, University of Ottawa, Ottawa, ON, Canada, [8]Department of Degenerative Neurological Diseases, National Institute of Neuroscience, National Center of Neurology and Psychiatry, Tokyo 187-8502, Japan and [9]Second Department of Neurology, University of Athens Medical School, Athens, Greece

Received October 19, 2011; Revised October 19, 2011; Accepted November 4, 2011

Genetic studies have implicated the neuronal ubiquitin C-terminal hydrolase (UCH) protein UCH-L1 in Parkinson's disease (PD) pathogenesis. Moreover, the function of UCH-L1 may be lost in the brains of PD and Alzheimer's disease patients. We have previously reported that the UCH-L1 polymorphic variant S18Y, potentially protective against PD in population studies, demonstrates specific antioxidant functions in cell culture. Albeit genetic, biochemical and neuropathological data support an association between UCH-L1, PD, synaptic degeneration and oxidative stress, the relationship between the dopaminergic system and UCH-L1 status remains obscure. In the current study, we have examined the dopaminergic system of mice lacking endogenous UCH-L1 protein (gracile axonal dystrophy mice). Our findings show that the lack of wild-type (WT) UCH-L1 does not influence to any significant degree the dopaminergic system at baseline or following injections of the neurotoxin methyl-4-phenyl-1,2,3,6-tetrahydropyridine (MPTP). Furthermore, using a novel intrastriatal adenoviral injection protocol, we have found that mouse nigral neurons retrogradely transduced with S18Y UCH-L1, but not the WT protein, are significantly protected against MPTP toxicity. Overall, these data provide evidence for an antioxidant and neuroprotective effect of the S18Y variant of UCH-L1, but not of the WT protein, in the dopaminergic system, and may have implications for the pathogenesis of PD or related neurodegenerative conditions, in which oxidative stress might play a role.

INTRODUCTION

The role of the abundant neuronal protein ubiquitin C-terminal hydrolase-L1 (UCH-L1) in the nervous system is uncertain. Inter-related functions as an ubiquitin C-terminal hydrolase, a stabilizer of free ubiquitin, an aberrant ubiquitin ligase, or a guardian of synaptic integrity, have been proposed (1–3). Gracile axonal dystrophy (*gad*) mice, harboring a spontaneous

*To whom correspondence should be addressed at: Division of Basic Neurosciences, Biomedical Research Foundation of the Academy of Athens (BRFAA) 4, Soranou Efesiou Street, Athens 11527, Greece. Tel: +30 2106597214, +30 2106597498; Fax: +30 2106597545; Email: lstefanis@bioacademy.gr (L.S.); mxilouri@bioacademy.gr (M.X.)
†Present Address: German Center for Neurodegenerative Diseases (DZNE), Bonn, Germany.

intragenic deletion of UCH-L1 (4), manifest sensory ataxia due to dying-back type of degeneration (5).

Parkinson's disease (PD) is now known to have a strong genetic component (6). One of the genes implicated in PD pathogenesis is the genetic locus PARK5 encoding UCH-L1. A missense mutation in UCH-L1, I93M, correlates with the autosomal dominant PD in a single family (7), while the polymorphism S18Y may be protective against the development of sporadic PD in several different ethnic groups (8–12). However, both findings have been questioned (13–21). The manner in which molecular variants of UCH-L1 may be associated with PD is unclear. The loss of the hydrolase activity (7), the toxic gain of function due to enhanced protein aggregation (22) or the enhancement of the aberrant ubiquitin ligase activity (23) have been proposed. Providing a further link to neurodegeneration, UCH-L1 is down-regulated and/or inactivated through oxidation in the brains of PD and Alzheimer's disease (AD) patients (24,25). Such a loss of function may be speculated, based on the above, to increase the vulnerability to synaptic degeneration. Conversely, indices of oxidative stress are elevated in *gad* mouse brains (26,27), and *gad* mice appear to exhibit vulnerability to lipid peroxidation (28). Exploring further the correlation between oxidative stress and UCH-L1, we previously showed that the putatively protective S18Y UCH-L1 variant, but not the wild-type (WT) protein, offers a specific protective effect against oxidative stress generated by hydrogen peroxide or cation 1-methyl-4-phenyl-pyridinium (MPP^+) in neuronal cultures (29).

Although, as mentioned, genetic, biochemical and neuropathological data point to a relationship between UCH-L1, PD, synaptic degeneration and oxidative stress, there has been little work on the study of the dopaminergic system, which suffers disproportionately in PD and is thought to be especially vulnerable to oxidative insults, in relation to the UCH-L1 status. In the current work, we have sought to examine the dopaminergic system of *gad* mice at baseline and following injections of the dopaminergic neurotoxin methyl-4-phenyl-1,2,3,6-tetrahydropyridine (MPTP), which induces death via oxidative stress (30). Furthermore, we have examined the effects of overexpression of WT and S18Y UCH-L1 on this system and found that only the S18Y polymorphism of UCH-L1 exerts neuroprotective properties *in vivo*.

RESULTS

Mice lacking endogenous UCH-L1 protein (*gad* mice) display similar vulnerability to MPTP-induced dopaminergic neurodegeneration

In order to examine the role of UCH-L1 in the integrity of the dopaminergic system at baseline conditions and following dopaminergic stress, we have used the *gad* mice, which have an intragenic deletion of *Uchl1* gene (4). We initially assessed baseline striatal tyrosine hydroxylase (TH) protein levels by western immunoblotting in *gad* mice at 12–16 weeks of age (just before the onset of the motor phenotype) and their corresponding controls (WT mice) ($n = 5$). We did not find any difference between the two groups using this method, which was also supplemented by western immunoblotting for TH or dopamine transporter (DAT), another dopaminergic terminal marker (Fig. 1A and B). Since DAT is a membrane-bound protein, it was detected mainly in the Triton-insoluble (sodium dodecyl sulfate (SDS) soluble) fractions.

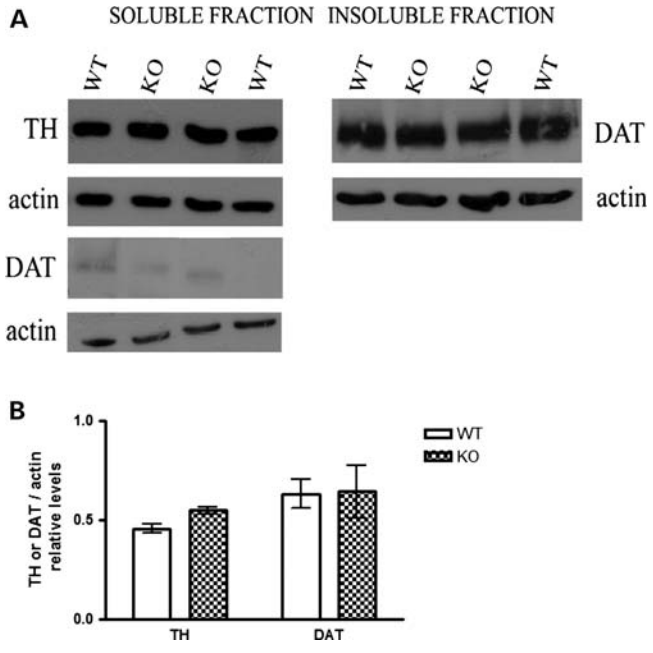

Figure 1. *Gad* and WT mice exhibit similar baseline striatal TH and DAT protein levels. (**A**) Representative western blots of TH and DAT protein levels in the striatum from 2-month-old *gad* (KO) and littermate WT mice. The striatum from WT and *gad* mice was dissected, homogenized and Triton soluble (30 μg protein) and insoluble (sodium dodecyl sulfate (SDS)-soluble 50 μg protein) extracts (prepared as described in Materials and Methods) were resolved by SDS–PAGE and immunoblotted for TH, DAT and β-actin (loading control). (**B**) Densitometry of striatal TH and DAT levels normalized against β-actin in western blots from *gad* (KO) and WT mice. Results are presented as mean ± SEM ($n = 5$). There were no significant differences noted.

To assess the potential differential effects of MPTP on striatal dopamine content depending on the UCH-L1 status, we exposed 8-week-old *gad* mice or their corresponding littermates (WT) to MPTP (30 mg/kg/day for 5 consecutive days) or equivalent volume of 0.9% saline, sacrificed the mice 2 weeks later and performed high-performance liquid chromatography (HPLC) analysis in striatal tissues ($n = 6$). Striatal levels of dopamine (DA) and its main metabolites, 3,4-dihydroxyphenylacetic acid (DOPAC) and homovanillic acid (HVA), were similar in saline-treated WT and *gad* mice, confirming a lack of an effect of loss of UCH-L1 on the dopaminergic system. Upon MPTP treatment, DA levels decreased significantly in both groups (57.86 ± 4.0% in the WT and 69.93 ± 3.8% in the *gad* mice) (Fig. 2A); similarly, MPTP evoked a significant decrease in the levels of DOPAC and HVA (Fig. 2B and C). Overall, there was no significant difference in the levels of DA and its metabolites between WT and *gad* mice following MPTP treatment (Fig. 2A–C).

We then went on to examine the striatal and nigral components of the nigrostriatal axis with TH immunohistochemistry. In the striatum, as expected, following the MPTP application, striatal TH fiber density decreased significantly and to the same level in both groups (Fig. 3A). To further assess the impact of UCH-L1 depletion on the dopaminergic system, we

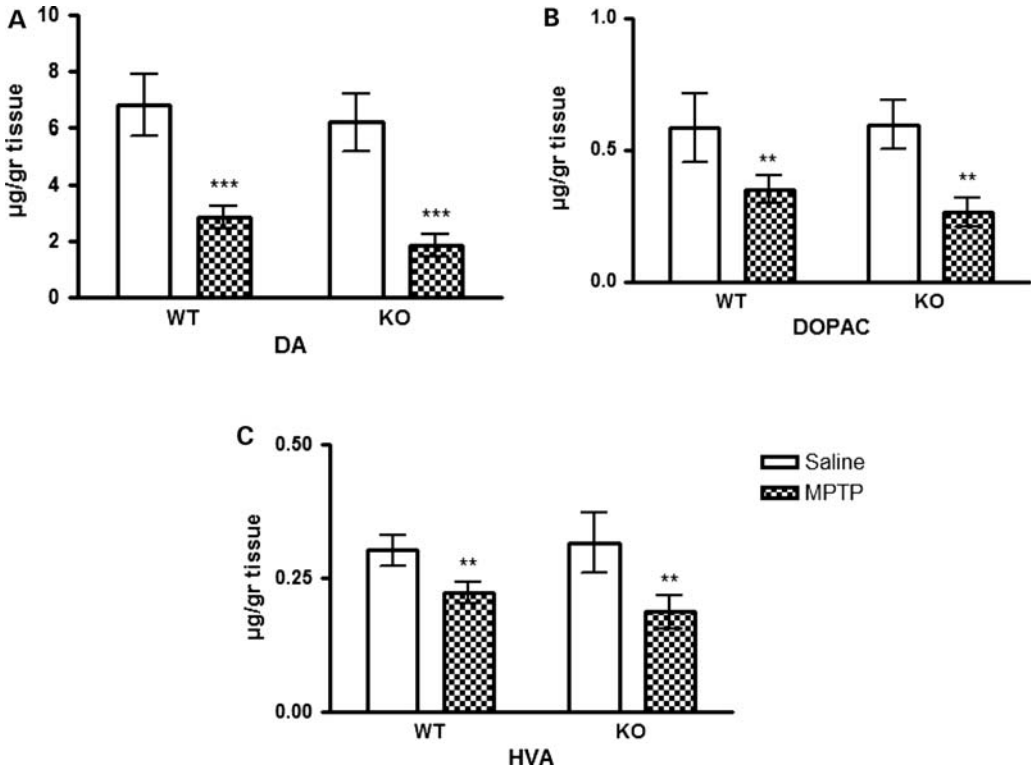

Figure 2. MPTP treatment evokes an analogous loss in striatal levels of DA and its main metabolites, DOPAC and HVA. WT or *gad* (KO) mice were treated with MPTP (30 mg/kg/day for 5 consecutive days) or 0.9% saline i.p. injections. Mice were sacrificed at 14 days after the first dose of MPTP and brains were collected as described in the protocol for HPLC determination of the levels of DA (**A**) and its metabolites DOPAC (**B**) and HVA (**C**). Bars represent mean ± SEM. Statistical analyses were carried out using two-way ANOVA (**$P < 0.01$, ***$P < 0.001$, compared between saline- and MPTP-treated mice). There was no statistical difference in the content of DA or its metabolites between MPTP-treated WT and *gad* mice.

counted the number of dopaminergic TH-positive neurons in the substantia nigra pars compacta (SNpc) using stereological methods. We found no difference between 8-week-old *gad* (KO) and littermate control (WT) mice, treated with saline (Fig. 3B and C). At 14 days post-MPTP treatment, both WT and *gad* mice manifested significantly decreased TH^+ neuron numbers ($n = 7$, 18.91 ± 5.1 and 27.67 ± 2.8% drop, respectively), compared with saline-treated controls. The numbers of TH-positive neurons post-MPTP treatment were not significantly different between WT and *gad* (KO) mice (Fig. 3B and C).

Taken together, our results show no dopaminergic deficit in *gad* mice at baseline. Moreover, *gad* mice displayed similar susceptibility to MPTP-evoked neurodegeneration compared with their littermate WT mice. These results indicate that *gad* mice are not differentially sensitive to the neurotoxin MPTP *in vivo* and that endogenous mouse UCH-L1 does not exert a significant antioxidant function in this system. If mouse UCH-L1 had possessed such a function, we would have expected its absence to lead to enhanced sensitivity to MPTP-induced death, as occurs for example in the case of the absence of the master regulator of antioxidant response Nrf2 (31).

Recombinant adenoviral (rAd) vectors are efficiently expressed in mouse striatum and SNpc following multiple intrastriatal injections

In our previous study, we have shown that S18Y, but not WT, UCH-L1, when expressed by transient lipofectamine-mediated transfection in neuronal cells, leads to a potent, specific (i.e. not observed against other insults), protection from MPP^+- and H_2O_2-induced reactive oxygen species (ROS) generation and death, thus linking this protective genetic variant to protection from oxidative stress (29). In order to extend these results to nigral neurons *in vivo*, we generated high-titer recombinant second-generation human serotype 5 adenoviral (rAd) vectors (32), encoding green fluorescent protein (GFP) or AdO (control vectors) and Flag-tagged WT or S18Y human UCH-L1.

Initially, to test whether such adenoviruses expressing WT or S18Y UCH-L1 would express these proteins in neuronal cells, and to examine whether the previously reported neuroprotective effects of S18Y UCH-L1 could be reproduced with this delivery system, we applied these viruses (100 multiplicity of infection (MOI) for each virus) to 7-day-old E18 rat cortical neurons, and 2 days later, exposed these cultures to 40 µM MPP^+, the active derivative of MPTP. These preliminary experiments also served to establish whether expression of S18Y UCH-L1 would be protective against MPP^+ toxicity in primary neurons, as this was previously demonstrated only in a neuronal cell line (29). In parallel immunostaining experiments, using the Flag antibody (for the UCH-L1 constructs), we have verified almost universal expression of the constructs in the infected cultures (Fig. 4A). None of the two UCH-L1-expressing viruses was toxic relative to EGFP virus on its own, as expected. Expression of rAd-S18Y, but not rAd-WT UCH-L1, was significantly protective against MPP^+

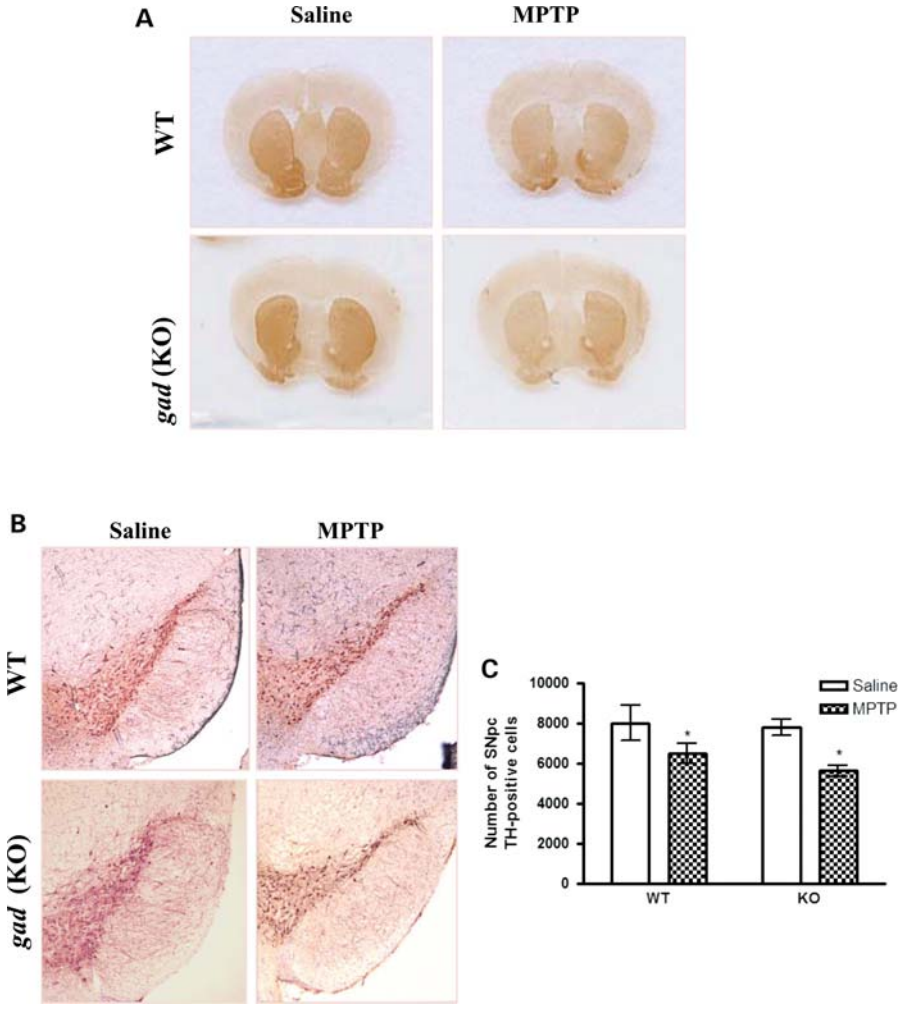

Figure 3. Immunostaining of TH-positive neurons in the striatum and the SNpc of WT and *gad* mice upon MPTP treatment. WT or *gad* (KO) mice ($n = 7$, per group and condition) were intoxicated with MPTP as in Figure 2 and 14 days after the first dose of MPTP, tissues were immunostained for TH following standard protocols. (**A**) Representative photomicrographs showing the effect of MPTP on TH immunostaining in the striatum of WT and *gad* mice, 14 days after the first MPTP injection. There was no statistical difference in striatal TH fiber density between MPTP-treated WT and *gad* mice. Scale bar: 200 μm. (**B**) Representative photomicrographs showing the loss of TH^+ neurons in the SNpc after MPTP treatment in WT and *gad* mice, 14 days after injection. Scale bar: 200 μm. (**C**) The number of TH^+ neurons in the SNpc of WT and *gad* mice treated with saline or MPTP was assessed using stereological methods ($n = 7$). Statistical analyses were carried out using two-way ANOVA ($^*P < 0.05$, compared between saline and MPTP-treated *gad* mice). There was no statistical difference in numbers of TH-positive neurons between MPTP-treated WT and *gad* mice.

toxicity, confirming that expression of S18Y UCH-L1 using this viral delivery system has neuroprotective effects (Fig. 4B and C). Notably, neuronal processes were remarkably preserved in the cortical cultures expressing S18Y UCH-L1 (Fig. 4B). These data confirm that the generated adenoviruses have the expected biological effects in cultured primary neurons.

We then went on to test whether these viruses would express the desired proteins *in vivo*, in the mouse substantia nigra. Adenoviral particles can be efficiently retrogradely transported to dopaminergic neurons within the SNpc following intrastriatal injections (33–35). We initially attempted to retrogradely overexpress these viruses in the mouse SNpc, after a single intrastriatal injection, using previously described protocols (35,36), but we could not detect expression of the transgenes within the SNpc (data not shown). To address this problem, we have established a novel, modified, more intense, protocol of adenoviral injections in the mouse striatum, adjusting recently published protocols in the rat (37).

Upon injection of a rAd-GFP or rAd-Flag (WT or S18Y UCH-L1) vector at four, instead of one, different sites (2 μl per site) in the mouse striatum, we observed a widespread distribution of rAd-GFP or rAd-Flag (WT or S18Y UCH-L1) virus around the injection sites (ipsilateral side), at 14 days after injection (Fig. 5A). The expression of the genes of interest was restricted to the side of injection, as no expression was detected contralaterally (Fig. 5A). Using this modified gene delivery tool, we have been able to consistently achieve an efficient transduction and robust Flag expression in $27.83 \pm 1.2\%$ of nigral dopaminergic neurons throughout the whole rostrocaudal axis of the SNpc, when assessed 2 weeks after viral injections by Flag labeling ($n = 3$). GFP nigral transduction was of a similar magnitude (Fig. 5B). Robust and equal

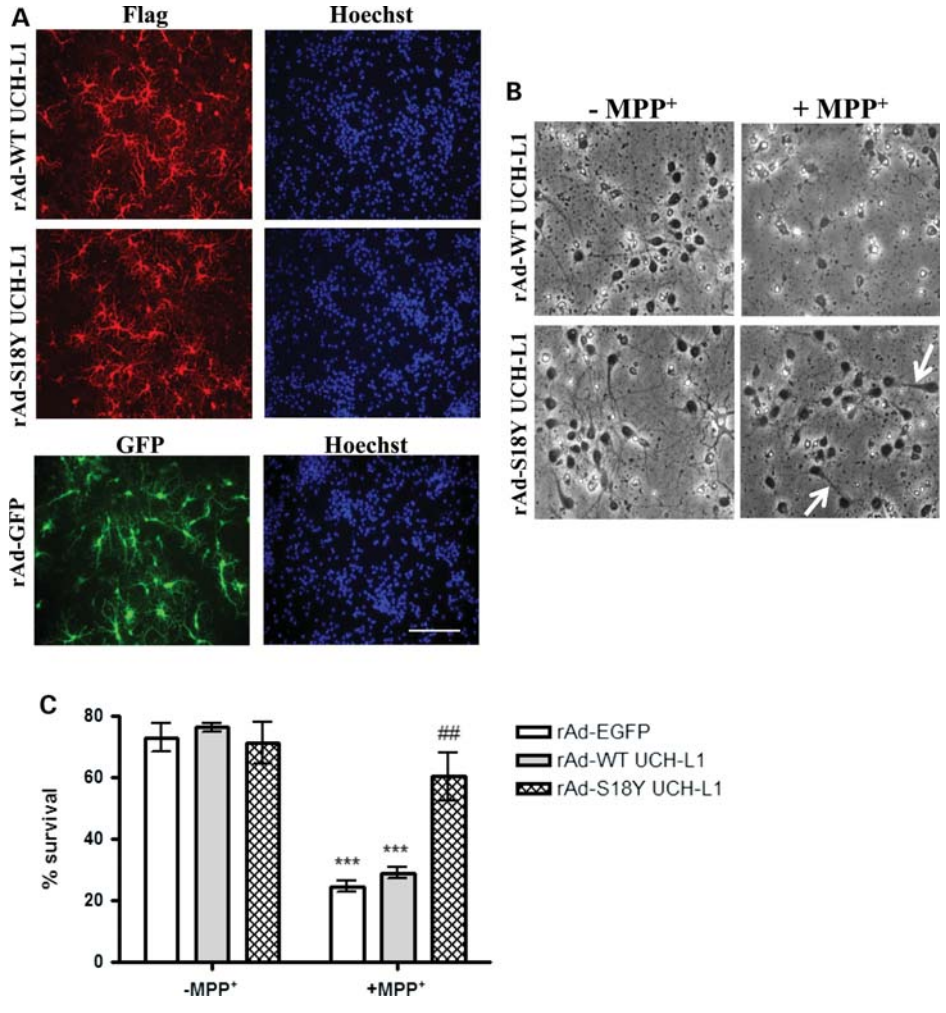

Figure 4. Expression of rAd virures and selective neuroprotective effect of the S18Y variant of UCH-L1 in primary rat cortical neurons. Seven-day-old E18 primary rat cortical neurons were transduced with rAd-WT or rAd-S18Y UCH-L1 (100 MOI for each virus) or the control virus rAd-GFP. Two days later, these cultures were exposed to 40 μM MPP^+ and 24 h later, the survival was assessed by counting the relative percentage of intact nuclei in each culture condition, compared with non-infected neurons. (**A**) Representative photomicrographs of rat cortical neurons 72 h post-transduction with the rAd-WT or rAd-S18Y UCH-L1 (flag tagged) or the control rAd-GFP virus. (**B** and **C**) MPP^+ administration evoked retraction of neuritic processes and neuronal death in cortical cultures. Only the cultures transduced with the rAd-S18Y UCH-L1 are protected from MPP^+-induced toxicity and preserve their neuritic processes [indicated by the arrows (B)]. Representative phase photomicrographs are shown in (B) and the percentage of survival 24 h after MPP^+ addition in each culture condition is shown in (C). The survival was assessed by counting the relative percentage of intact nuclei in each culture condition, compared with non-infected neurons. The data are presented as mean ± SEM of three independent experiments. Statistical analyses were performed using one-way ANOVA followed by the Newman–Keuls *post hoc* test [$^{***}P < 0.001$, compared between cultures treated with MPP^+ and control ($-MPP^+$) cultures; $^{\#\#}P < 0.01$, compared between rAd-S18Y and rAd-WT UCH-L1 or the control rAd-GFP-transduced cultures treated with MPP^+].

expression of the genes of interest in the striatum and the ventral midbrain of injected mice was further verified by western immunobloting (Fig. 5C), 14 days after injection ($n = 3$). In the ipsilateral striatum of animals injected with rAd-WT or rAd-S18Y UCH-L1, we observed that both variants were expressed at comparable levels with the endogenous protein (Fig. 5C, 6th row). The overexpressed protein is migrating higher on the gel because of the Flag-tag, compared with the endogenous protein. This was not so obvious in the ventral midbrain tissue, due to the high abundance of the UCH-L1 protein in this brain region and the close proximity of the endogenous and overexpressed UCH-L1 bands. On the contrary, the expression of both UCH-L1 variants in the ventral midbrain of rAd-WT or S18Y UCH-L1 injected animals was apparent when membranes were probed with anti-Flag antibody, which recognizes only the overexpressed protein (Fig. 5C, 5th row). Additionally, as shown in Figure 5C, GFP adenoviral delivery was accompanied by a significant loss of TH immunolabeling in the striatum and in the SNpc, while both rAd-Flag (WT or S18Y UCH-L1) viruses were not toxic, as manifested by TH detection. For this reason, we chose to use the rAd-AdO (empty vector) instead of rAd-GFP virus for subsequent experiments with MPTP intoxication.

In order to ensure that, following this modified protocol of striatal adenoviral injections, we would achieve meaningful, but close to the physiological range, levels of overexpression of UCH-L1 in the dopaminergic neurons of the SNpc, we

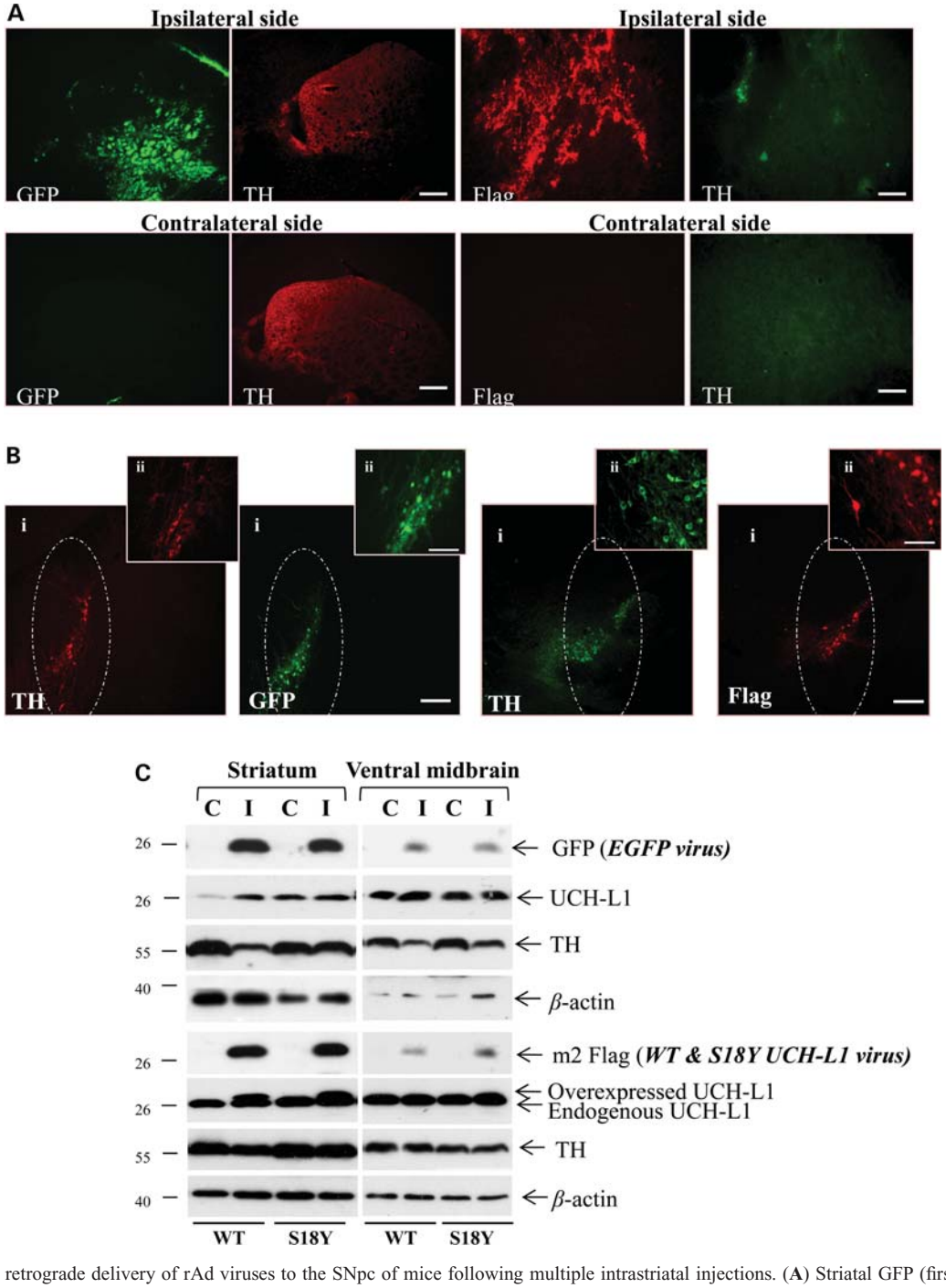

Figure 5. Selective retrograde delivery of rAd viruses to the SNpc of mice following multiple intrastriatal injections. (**A**) Striatal GFP (first column) and Flag (third column), combined with TH (second and fourth columns) immunostaining ipsilateral (top row) and contralateral (bottom row) to the adenoviral injections, 14 days post-striatal injection. Scale bar: 500 μm. (**B**) Ventral midbrain sections from mice injected as in (A) were co-immunostained with TH and GFP (top row), or TH and Flag (bottom row), and representative photomicrographs were obtained. The boundaries of SNpc are depicted with the white landmark. Scale bars: panel (i), 200 μm; panel (ii), 50 μm. (**C**) Western blot analysis of GFP and Flag-UCH-L1 expression in the striatum and the ventral midbrain, at the contralateral (*C*) and the Ipsilateral (*I*) side of the injection. rAd-WT UCH-L1-Flag, rAd-S18Y UCH-L1-Flag and rAd-GFP-injected animals were sacrificed at 14 days after injection ($n = 3$ per group). Protein extracts from each sample were subjected to SDS gel electrophoresis and membranes were probed with anti-GFP, anti-Flag, anti-UCH-L1, anti-TH and anti-β-actin antibodies (loading control).

assessed levels of UCH-L1 in transduced (Flag-positive) neurons, and compared them with endogenous UCH-L1 (Flag-negative) levels in neighboring nigral neurons. To first test the specificity of the UCH-L1 staining within the dopaminergic neurons of the SNpc, we used nigral sections from WT and *gad* mice, which lack the endogenous UCH-L1 protein and represent the ideal negative control for the staining. Double immunostaining for TH and UCH-L1 revealed a specific

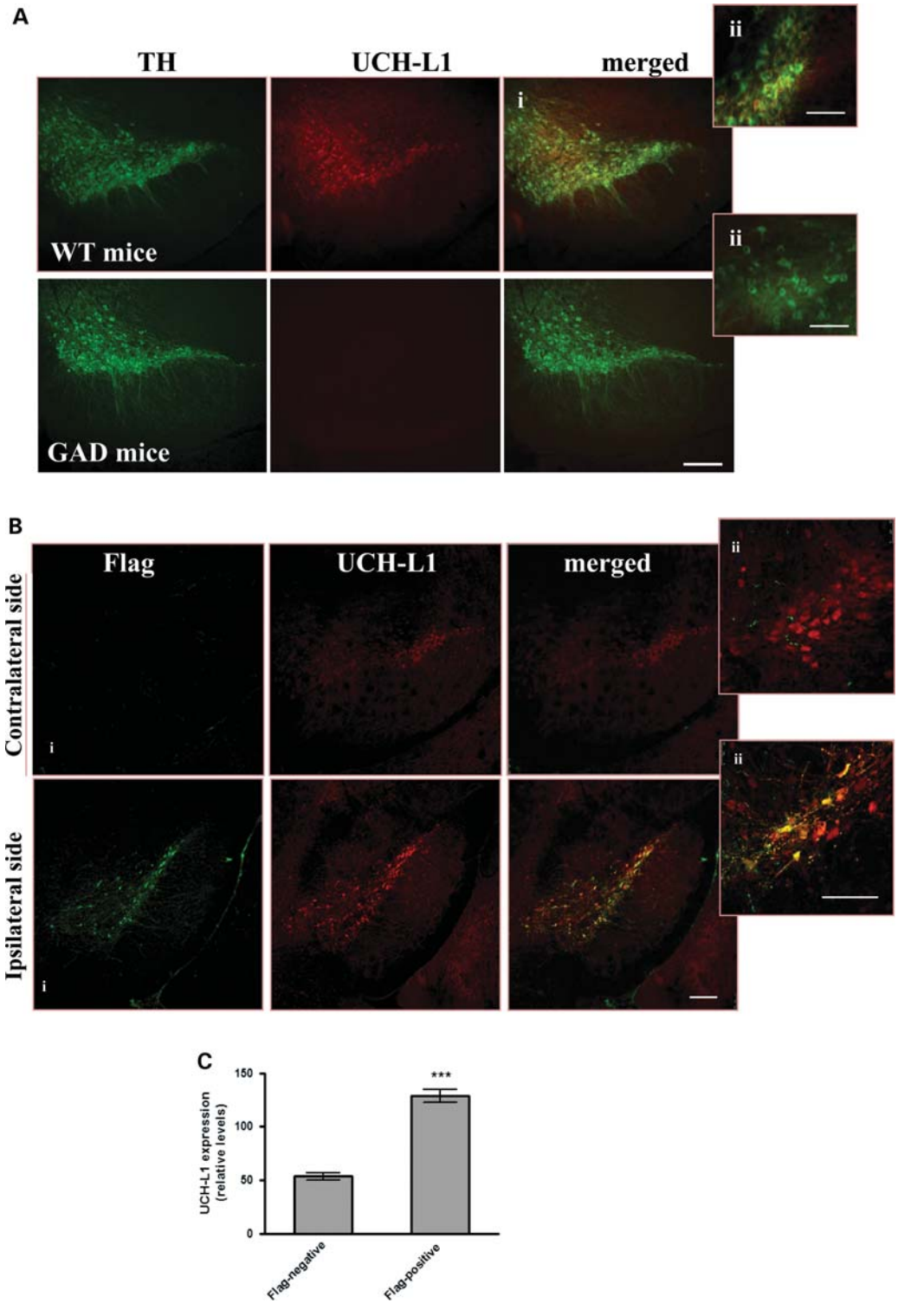

Figure 6. Analysis of the UCH-L1 (endogenous and overexpressed) expression in the mouse SNpc, following multiple intrastriatal injections. (**A**) Immunohistochemical staining for TH (first column) and UCH-L1 (second column) on coronal brain sections of the SNpc from WT (top row) and *gad* (bottom row) mice. Low (i) and high (ii) power merged images are shown in the third column. Scale bars: panel (i), 100 μm; panel (ii), 50 μm. (**B**) Mice were injected with rAd-S18Y UCH-L1-Flag and 14 days later ventral midbrain immunohistochemistry was performed with anti-Flag (first column) and anti-UCH-L1 (second column) antibodies on the ipsi- (bottom row) or contralateral side (top row). Merged images are shown on the right. Low (i) and high (ii) power merged images are shown. Scale bar: panel (i), 200 μm; panel (ii), 50 μm. (**C**) Measurement of UCH-L1 fluorescence intensity in Flag-negative and -positive neurons in the SNpc of animals in (B) was performed with the use of Image J software, as described in Materials and Methods. Statistical analyses were carried out using one-way ANOVA followed by the Newman–Keuls *post hoc* test (***$P < 0.001$, compared between uninduced and Flag$^+$-transduced SNpc neurons of rAd-S18Y-UCH-L1-Flag-injected animals).

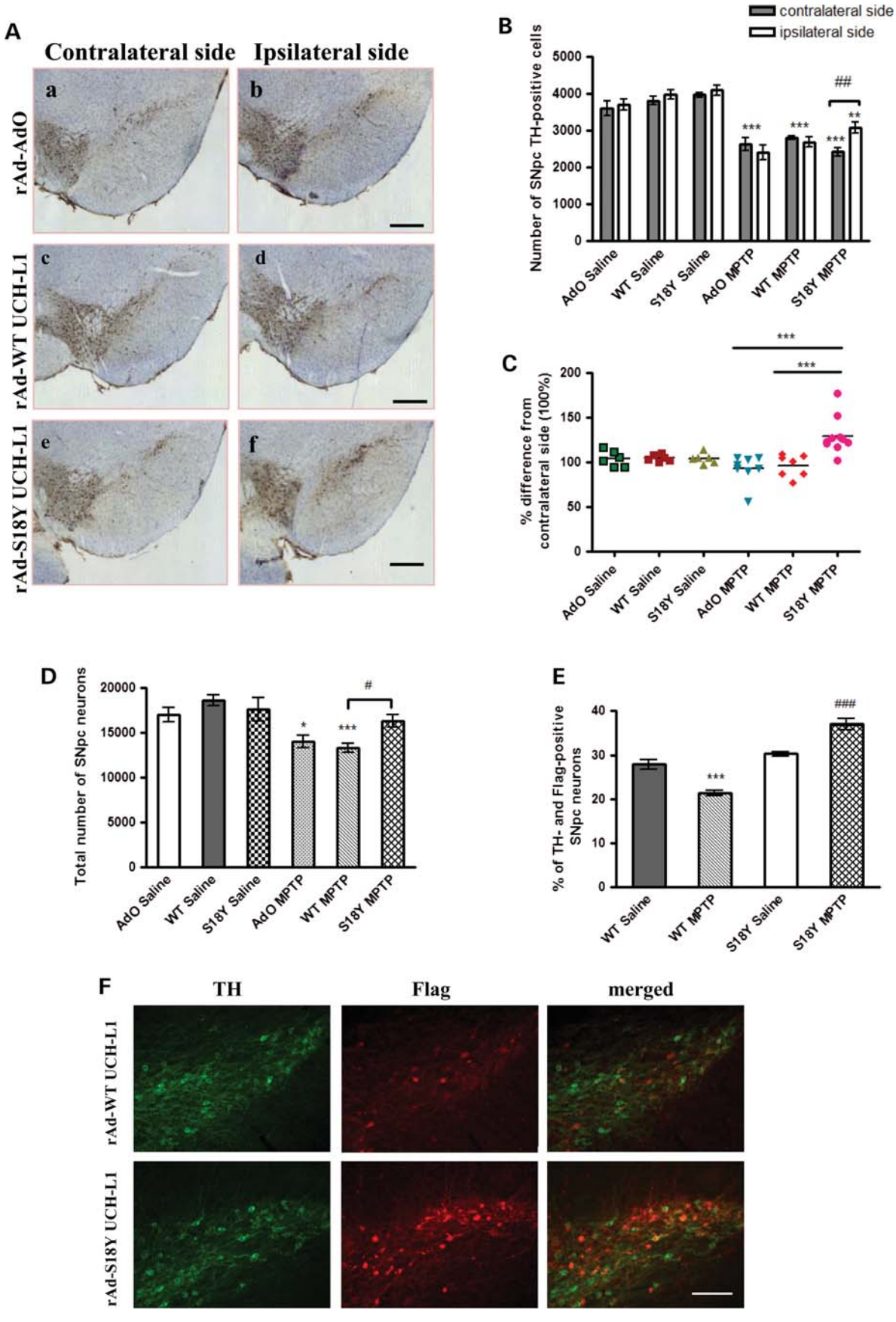

UCH-L1 immunoreactivity within the cell soma, including the nucleus, of TH^+ neurons of the SNpc (Fig. 6A). Subsequently, we assessed the levels of the overexpressed Flag-tagged UCH-L1 relative to the endogenous protein levels. Confocal microscopy for UCH-L1 and Flag and quantitative fluorescence analysis using the Image J software revealed that, in SNpc transduced neurons, the levels of expression of UCH-L1 were increased by ~2–3-fold above the endogenous levels (Fig. 6B and C). This means that the overexpressed protein is present in amounts of ~1–2-fold above endogenous. Of note, immunolabeling of overexpressed UCH-L1, in contrast to that of the endogenous protein, was also present within axonal processes. It should also be noted that this robust, but close to the physiological levels, induction of UCH-L1 that we achieve at the single-cell level only in transduced dopaminergic neurons is significantly diluted at the level of the total ventral midbrain, which we sample for western immunoblots in Figure 5C, hence the lack of perceptible induction over background in the latter case.

MPTP-induced neuronal loss is attenuated by adenoviral expression of S18Y UCH-L1

To investigate whether S18Y UCH-L1 could protect against MPTP injections *in vivo*, we overexpressed S18Y UCH-L1 in the SNpc of mice, using the modified protocol described above, expressing either rAd-S18Y or rAd-WT UCH-L1, or rAd-AdO (control virus). Seven days after the striatal viral injections, mice were subjected to MPTP (18 mg/kg/four injections per day, 2 h apart) or equivalent volume of 0.9% saline. We chose to use this rather acute protocol in order to: (a) achieve a higher percentage of cell death in the SNpc (compared with ~20% TH^+ neuron death that we achieved with the MPTP regimen we utilized for the analysis of the dopaminergic system of the *gad* mice) and (b) avoid the confound of toxicity induced by the adenoviral transduction itself over time. The neuroprotective effect of the S18Y polymorphism of UCH-L1 in the mouse dopaminergic system was initially estimated by stereological cell counting of TH^+-positive neurons in the SNpc of mice injected with the rAd-WT UCH-L1, rAd-S18Y UCH-L1 or rAd-AdO virus. In particular, comparing ipsi- to contralateral side of viral injection, only rAd-S18Y UCH-L1-injected mice showed a significant protection ($29.05 \pm 6.5\%$, $n = 10$) against MPTP-mediated loss of nigral TH^+ neurons (Fig. 7A–C). This protection at the level of the total population of dopaminergic neurons was impressive, given the fact that only 27.8% of these neurons were transduced with S18Y UCH-L1 (see above). In fact, considering a mean of ~40% TH neuron loss with the current regimen (Fig. 7B) and this transduction efficiency, one would expect, if S18Y UCH-L1 was 100% effective in suppressing TH neuron loss in each neuron it was expressed an enhanced survival of $27.8 \times 40\%$ of the total population of TH neurons, i.e. 11.1%, which is very close to what we observe (Fig. 7B). Therefore, given the limits of transduction efficiency with the current protocol, the protective effect of S18Y UCH-L1 is robust. Importantly, and in agreement with our findings in MPP^+-treated cortical neurons (Fig. 4B), overexpression of S18Y UCH-L1 resulted in substantial preservation of the dendrites of the SNpc TH^+ neurons that project in the pars reticulata, compared with the animals injected with the WT protein or the control AdO (Fig. 7A). To further confirm these results, we also performed western immunoblot analysis. This revealed a statistically significant preservation of TH protein levels in the ipsilateral side of mice injected with the rAd-S18Y UCH-L1 virus (Supplementary Material, Figure S1).

Counting the total SNpc neurons (TH and Nissl-positive), we also observed a significant increase in the total number of SNpc neurons in the ipsilateral side of rAd-S18Y injected animals upon MPTP treatment (Fig. 7D). Moreover, counting of the percentage of nigral neurons that remain Flag positive upon MPTP treatment showed a significant drop in the

Figure 7. Adenoviral mediated expression of the S18Y variant of UCH-L1 protects against MPTP-induced nigral cell loss. Mice were injected unilaterally in the striatum with rAd-AdO, rAd-WT or rAd-S18Y UCH-L1 and 7 days later were treated with MPTP (18 mg/kg/four injections per day, 2 h apart) or 0.9% saline. Animals were sacrificed 7 days following MPTP treatment and tissues were immunostained for TH and Nissl or TH and Flag, according to standard protocols. (**A**) Representative SNpc photomicrographs of MPTP-treated mice injected with the adenoviruses expressing rAd-AdO (top row, *a, b*), rAd-WT UCH-L1 (middle row, *c, d*) or rAd-S18Y UCH-L1 (bottom row, *e, f*), showing the loss of TH^+ neurons upon MPTP treatment. The contralateral hemisphere served as the non-injected, MPTP-treated control. Only in the rAd-S18Y UCH-L1-injected animals, there is a significant preservation of TH^+ neurons in SNpc and their dendrites in the reticulata, upon MPTP treatment in the ipsilateral side (*f*), when compared with non-injected contralateral side (*e*) of the same mouse. Sections are counterstained with Nissl (blue) for anatomical reference.Scale bar: 200 μm. (**B**) Quantification of numbers of TH^+ neurons in the contralateral and ipsilateral side of the SNpc of all animals in the groups. Data are presented as mean ± SEM ($n = 6$/group for saline, $n = 7–10$/group for MPTP-treated animals). Statistical analyses were carried out using one-way ANOVA followed by the Newman–Keuls *post hoc* test ($^{**}P < 0.01$, $^{***}P < 0.001$ comparing between saline to MPTP-treated animals; $^{\#\#}P < 0.01$, comparing between the contralateral to ipsilateral side in rAd-S18Y UCH-L1-injected animals upon MPTP treatment). (**C**) Stereological quantification of the percentage loss of TH^+ neurons in the SNpc of rAd-AdO, rAd-WT UCH-L1 and rAd-S18Y UCH-L1-injected animals ($n = 6$/group for saline, $n = 7–10$/group for MPTP-treated animals). Data are expressed as percentage of difference from the contralateral side (100%). Statistical analyses were carried out using one-way ANOVA followed by the Newman–Keuls *post hoc* test ($^{***}P < 0.001$, compared between the rAd-S18Y UCH-L1 and rAd-AdO or rAd-WT UCH-L1-injected animals, baseline corrected). (**D**) Quantification of numbers of TH-positive and Nissl-stained neurons in the ipsilateral side of the SNpc of all animals in the groups. Data are presented as mean ± SEM ($n = 6$/group for saline, $n = 7–10$/group for MPTP-treated animals). Statistical analyses were carried out using one-way ANOVA followed by the Newman–Keuls *post hoc* test ($^{*}P < 0.05$, $^{***}P < 0.001$ compared between saline and MPTP-treated animals; $^{\#}P < 0.05$, comparing between the ipsilateral side of rAd-S18Y UCH-L1 and rAd-WT UCH-L1 or rAd-AdO-injected animals upon MPTP treatment). (**E** and **F**) Quantification of TH- and Flag-positive neurons in the ipsilateral side of the SNpc of animals injected with rAd-WT or rAd-S18Y UCH-L1 with the use of Image J software, as described in Materials and Methods. Statistical analyses were carried out using one-way ANOVA followed by the Newman–Keuls *post hoc* test ($^{***}P < 0.001$, compared between saline and MPTP-treated mice; $^{\#\#\#}P < 0.001$, comparing between the rAd-S18Y and rAd-WT UCH-L1-injected animals upon MPTP treatment). (F) Representative immunohistochemical staining for TH (first column) and Flag (second column) on the ipsilateral side of the SNpc from rAd-WT (top row) and rAd-S18Y (bottom row) UCH-L1-injected mice, upon MPTP treatment. Merged images are shown on the third column. Scale bar: 50 μm.

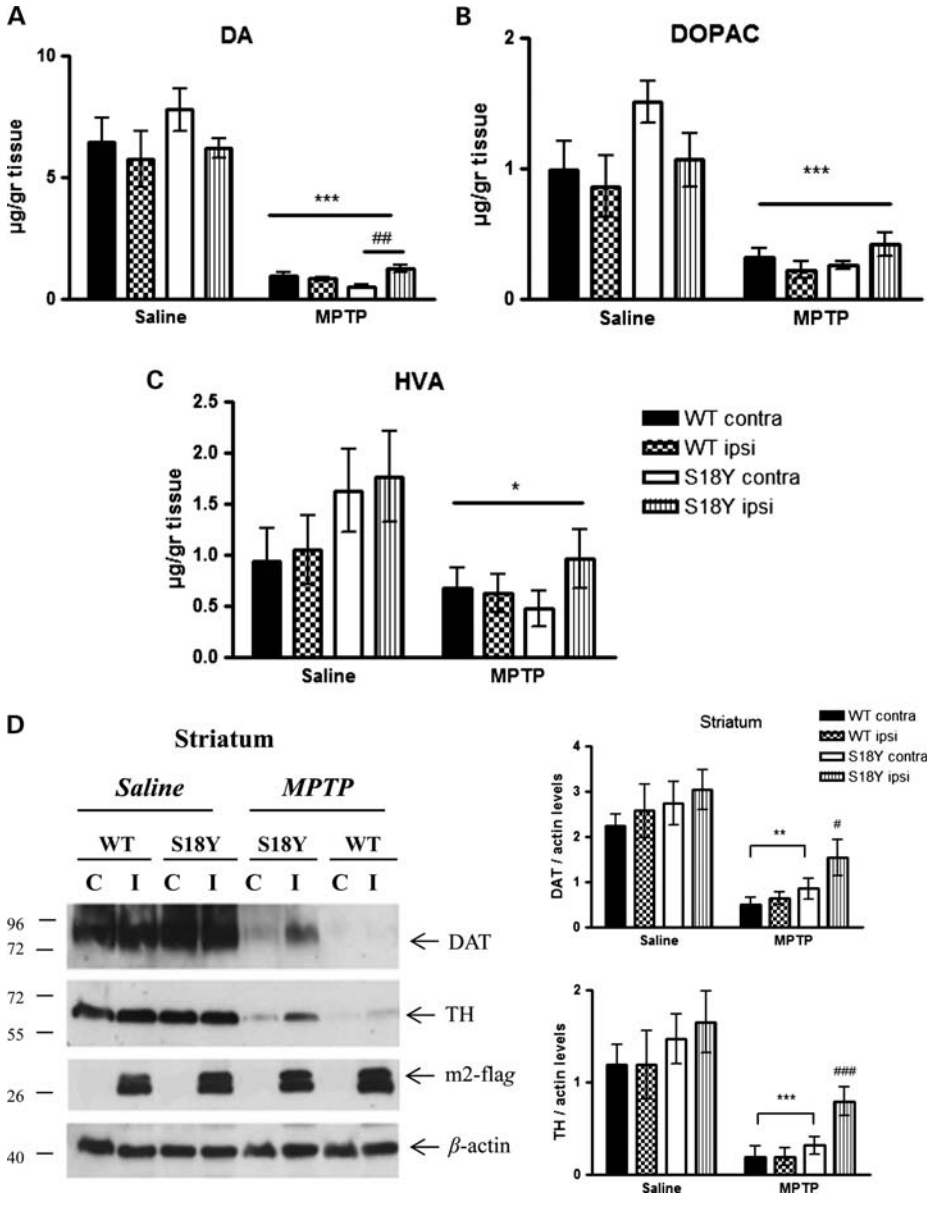

Figure 8. Adenoviral-mediated expression of the S18Y variant of UCH-L1 preserves striatal DA content and TH protein levels upon MPTP-induced intoxication. Mice were injected unilaterally in the striatum with rAd-WT or rAd-S18Y UCH-L1 as above. Seven days later, animals were treated with MPTP (18 mg/kg/four injections per day, 2 h apart) or 0.9% saline. Mice ($n = 5$ per group) were sacrificed 7 days later and striatal levels of DA (**A**) and its metabolites DOPAC (**B**) and HVA (**C**) were determined as in Figure 2. Bars represent mean ± SEM. Statistical analyses were carried out using one-way ANOVA ($^{*}P < 0.05$, $^{***}P < 0.001$, compared between saline and MPTP-treated mice). rAd-S18Y UCH-L1 injected mice showed higher levels of DA and metabolites upon MPTP treatment ($^{**}P < 0.01$, Student's *t*-paired test, compared between the contralateral and the ipsilateral side of rAd-S18Y UCH-L1-injected animals upon MPTP treatment). (**D**) Western blot analysis of the striata used in the HPLC measurements above ($n = 5$ per group). Protein extracts from the contralateral (*C*) and the Ipsilateral (*I*) side of the injection were subjected to SDS–PAGE and membranes were probed with anti-DAT, anti-TH, anti-Flag and anti-β-actin antibodies (loading control). Representative immunoblots are shown on the left panels and quantitative densitometric analysis of striatal DAT and TH levels normalized against β-actin are shown on the right panels. All presented data are expressed as mean ± SEM. Statistical analyses were carried out using one-way ANOVA followed by the Newman–Keuls *post hoc* test ($^{**}P < 0.01$, $^{***}P < 0.001$, compared between saline and MPTP-treated mice; $^{\#}P < 0.05$, $^{\#\#\#}P < 0.001$, compared between the contralateral and ipsilateral side of rAd-S18Y UCH-L1-injected animals upon MPTP treatment).

percentage of $TH^{+}/Flag^{+}$ neurons in rAd-WT UCH-L1 injected animals (21.32 ± 0.6%, compared with 27.84 ± 1.2%, in the saline-treated animals), indicating that some of the compromised, but not yet dead, TH^{+} neurons preferentially lose their Flag staining (Fig. 7E and F). On the contrary, the rAd-S18Y UCH-L1-injected animals not only maintain their Flag staining upon MPTP treatment, but they actually increase it above baseline (36.9 ± 1.2%, compared with 30.2 ± 0.5%, in the saline-treated animals), indicating that the TH^{+} neurons expressing Flag-S18Y UCH-L1 are preferentially protected (Fig. 7E and F).

In order to investigate the effects of S18Y UCH-L1 on the dopaminergic terminals, mice were unilaterally injected with the rAd-WT or rAd-S18Y UCH-L1 and 7 days later were

exposed to MPTP (18 mg/kg/four injections per day, 2 h apart) or saline, as above ($n = 5$). Upon MPTP treatment, DA levels decreased significantly in all groups (Fig. 8A). Comparing contralateral to ipsilateral sides, in the rAd-WT UCH-L1-injected mice, DA levels dropped robustly in a similar magnitude ($85.85 \pm 1.0\%$ in the contralateral and $85.77 \pm 1.2\%$ in the ipsilateral side), whereas in the rAd-S18Y UCH-L1-injected mice, the reduction in DA levels in the ipsilateral side was significantly lower ($80.02 \pm 0.81\%$) compared with that in the contralateral side ($93.52 \pm 0.38\%$) (Fig. 8A). Similar results were obtained for the levels of DOPAC and HVA (Fig. 8B and C). Western immunoblot analysis in the same striata used for the HPLC analysis revealed a significant preservation of DAT and TH protein levels in the ipsilateral side of mice injected with the rAd-S18Y UCH-L1 upon MPTP treatment (Fig. 8D). No differences were observed between contralateral and ipsilateral sides of mice injected with the rAd-WT UCH-L1 virus.

DISCUSSION

In the current manuscript, we have attempted to extend our previous results regarding the neuroprotective role of the polymorphic variant S18Y of UCH-L1, obtained in cell culture (29), to the *in vivo* level. We have found that mouse nigral neurons transduced with S18Y UCH-L1, but not the WT protein, are significantly protected against MPTP toxicity. This effect was evident in the nigral cell bodies and in the nigrostriatal terminals. Given the fact that $<30\%$ of nigral neurons were transduced, it appears that the majority of such neurons are protected. This underscores the potent effect of the expression of this polymorphic variant of UCH-L1 on neuronal survival against this classical dopaminergic neurotoxin. MPTP is known to exert its neurotoxic effects on nigral neurons through mitochondrial damage and subsequent activation of oxidative stress (30,38). Given the ability of S18Y UCH-L1 in cell culture to selectively protect against insults that induce oxidative stress, such as MPP^+ or hydrogen peroxide, but not against other insults, and its ability to significantly diminish ROS generation (29), it is reasonable to assume that the *in vivo* neuroprotective effect of this polymorphic variant is due to its antioxidant properties.

It is important to note that the neuroprotective effect of S18Y UCH-L1 was achieved with the levels of expression of the transgene that were $\sim$1.5-fold over endogenous UCH-L1 levels in nigral neurons. Although ideally, to simulate the heterozygote or homozygote S18Y UCH-L1 state in humans, levels should be increased above endogenous by 50 or 100%, respectively, levels in our experiments were close to a physiological range. It can be assumed then that humans harboring this polymorphic variant should be protected against oxidative stress injury to the nervous system, and in particular to nigral neurons, *in vivo*. The data however regarding the protective effect of S18Y UCH-L1 against the development of PD are conflicting (8–13). In our own recent study in a Greek cohort, we failed to find a significant association between any polymorphic variant of the UCH-L1 gene, including S18Y, and the PD status (39). There may be various reasons for the discrepancy between the observed selective neuroprotective effects of S18Y UCH-L1 against oxidative stress insults and the apparent lack of an association of this polymorphism with PD in some case–control studies. We favor the possibility that the role of oxidative stress in PD pathogenesis (and, correspondingly, the influence of the presence of S18Y UCH-L1) may be relatively minor in most populations, and may be relevant to only specific subgroups, such as, for example, patients with homozygous loss of function mutations in DJ-1 (40–43). Indeed, recent genome-wide association study (GWAS) have identified a number of genetic loci associated with sporadic PD, and none of them encode genes relevant to oxidative stress pathways (6,44,45). In contrast, the locus synuclein-alpha, encoding for alpha-synuclein, is significantly associated with PD in multiple independent GWAS (6,44,46). Interestingly, preliminary results from our laboratory indicate that S18Y UCH-L1 is not protective against alpha-synuclein-induced neurodegeneration (Kyratzi *et al.*, unpublished results), consistent with the idea that the process of oxidative stress may not play a major role in synucleinopathies. It is conceivable however that the S18Y status would have a much more profound influence on processes more definitively associated with oxidative stress, such as aging. Another issue that deserves further study is the potential of S18Y UCH-L1 to modify the course of PD, as the evolution of the disease, and not its initial pathogenesis, may be more dependent on oxidative stress pathways.

The nature of the putative anti-oxidant function of S18Y UCH-L1 is unknown, but one could speculate that, given the propensity of UCH-L1 to attach to membranes when farnesylated (47), it may exert such functions at the level of the mitochondrial membrane. Experiments addressing this issue are under way in our laboratory.

Both AD and PD are associated with decreased expression and/or inactivation of UCH-L1, and, consequently, it has been postulated that such a loss of function of UCH-L1 may be relevant to disease pathogenesis (24,25). Consistent with this idea, synaptic dysfunction, alterations in synapse morphology and frank synaptic or neuronal terminal degeneration may occur as a consequence of UCH-L1 loss or inhibition (5,48–50). In our own experiments, we have not detected any obvious untoward consequences in nigral neurons or their dopaminergic terminals from the lack of endogenous UCH-L1 either at baseline, or following application of the mitochondrial neurotoxin MPTP, which induces death through ROS activation. To our knowledge, this is the first study that has systematically assessed the dopaminergic system in *gad* mice. It is notable that UCH-L1, a very abundant protein in the central nervous system, is expressed at especially high levels in the ventral midbrain, and, within this area, is localized to a large extent within dopaminergic neurons (Fig. 6A). UCH-L1 has been linked to both pro-survival and pro-death pathways (51–53). Its role in nigral neurons remains to be elucidated, but, from our own experiments, it appears that it is dispensable for their survival and dopaminergic phenotype. Consequently, the loss of function of UCH-L1 is unlikely to represent a major part of PD pathogenesis. The lack of effect of overexpressed human WT UCH-L1 in our previous cell culture experiments (29), and on the dopaminergic system at baseline and following MPTP-induced neurotoxicity, presented here, is also consistent with this idea.

From a technical point of view, our modified protocol has enabled us to achieve significant transduction of mouse nigral neurons through intrastriatal adenoviral injections. Importantly, with our approach, nigral transduction was achieved through the whole rostro-caudal extent of the nigra, enabling stereological analysis. Although the efficiency of viral transduction was incomplete within the mouse nigra, it was sufficient to observe a biologically relevant effect. This protocol could be further improved with the use of neuronal-specific promoters, as in the case of Dusonchet *et al.* (37), who used a similar approach in rats. With our protocol, no obvious neurotoxic effects were seen at the levels of terminals or cell bodies with the various transgenes expressed, with the notable exception of EGFP adenoviral injections, which caused a significant drop in TH immunoreactivity in both striatum and nigra (Fig. 5C); for this reason, this adenovirus was not used in further experiments.

In conclusion, we demonstrate, using a modified adenoviral transduction protocol, that nigral overexpression of S18Y UCH-L1 leads to significant protection from MPTP-induced neurotoxicity, extending previous results achieved in cell culture systems and providing further evidence for a potent antioxidant and neuroprotective effect of this common polymorphic variant. In contrast, the loss of endogenous UCH-L1 or overexpression of its human WT counterpart had no effect on the dopaminergic system. These results have implications for at least certain subtypes of PD and for other neurodegenerative conditions in which oxidative stress is thought to play a role.

MATERIALS AND METHODS

Animals

The *gad* mice with an intragenic deletion in the gene encoding ubiquitin C-terminal hydrolase (UCH-L1) and their littermate control (WT) mice were used. The generation and phenotype of *gad* mice has been described previously (4). Heterozygote breeding pairs of +/− *gad* mice, originating from the laboratory of Dr Keiji Wada (National Institute of Neuroscience, Tokyo, Japan), were housed in the animal facility of the Biomedical Research Foundation of the Academy of Athens (BRFAA) in a room with a controlled light–dark cycle (12 h light–12 h dark) and free access to food and water. Genotyping of heterozygote +/− (hets), +/+ (WT) and −/− (*gad*/*gad*, KO) mice was performed by polymerase chain reaction (PCR) with genomic DNA extracted from tails, as described with minor modifications (4). For the adenoviral injections, 8-week-old male C57BL/6 mice (20–25 g) were used. All efforts were made to minimize animal suffering and to reduce the number of the animals used, according to the European Communities Council Directive (86/609/EEC) guidelines for the care and use of laboratory animals. All animal experiments were approved by the Institutional Animal Care and Use Committee of BRFAA.

Adenoviral vector construction and virus production

The UCH-L1 polymorphic variant flag-Ser18Tyr UCH-L1 was generated by PCR-mediated site-directed mutagenesis of full-length human flag-WT UCH-L1, as previously described (29). These cDNAs were cloned into a modified version of the PENTR.GD entry vector and introduced into the pAd/PL-DEST Gateway vector (Invitrogen). Second-generation E1, E3, E2a-deleted recombinant human serotype 5 adenoviruses (rAd) were generated, as described previously (54). Viral vector stocks were amplified from plaque isolates in order to guarantee homogeneity of the production. Final vector stocks were purified and concentrated using double discontinuous and continuous cesium chloride (CsCl) gradients. Viral titers of purified vector stocks were determined by Adeno-X Rapid Titer kit (Clontech) and (optical density) OD_{260} measurements. The following titers were obtained, expressed as viral particles (vp)/μl: 7.5×10^8 for rAd-WT UCH-L1, 5.64×10^8 for rAd-S18Y UCH-L1, 7.8×10^8 for rAd-AdO and 1.43×10^9 for rAd-GFP.

Stereotaxic unilateral injections into the mouse striatum

For stereotaxic injections adult C57/Bl6 male mice (8 weeks of age) (Charles River Laboratories, L' Arbresle Cedex, France), weighing ∼20–25 g were deeply anesthetized with a mixture of xylazine/ketamine and placed in the stereotaxic frame (David Kopf Instruments, Tujunga, CA, USA). Recombinant Ad vectors were injected unilaterally in the right striatum at four points, corresponding to two deposits along two needle tracts at the following anterior–posterior (AP), medio-lateral relative to bregma, dorso-ventral relative to skull surface coordinates: 0.5/−2.2/−3.4 and −3.2; 0.5/−1.5/−3.4 and −3.6. Two microliters of virus at a concentration of 4×10^7 vp/μl were injected per site using a 10-μl Hamilton syringe with a 34-gauge blunt tip needle at a speed of 0.5 μl/min, with an automatic pump (Univentor, Malta). The more ventral site in each needle tract was injected first and the needle was left in place for 5 min before slowly moving to the more dorsal site in the same needle tract, after injection of which the needle was left for an additional 10 min before slowly being withdrawn.

MPTP administration

Two different MPTP dosing regimens were used, as described previously (55). For the phenotypic characterization of the dopaminergic system of *gad* mice, a *sub-acute* or *chronic* intoxication regimen corresponding to one injection per day for 5 consecutive days was used. Mice received one intraperitoneal (i.p.) injection of MPTP–HCl per day (30 mg of free base per kg of body weight per injection; Sigma, St. Louis, MO, USA) for 5 consecutive days. Mice were sacrificed 14 days after the first MPTP injection. For the study of the neuroprotective effects of the S18Y variant of UCH-L1, an *acute* intoxication was utilized, encompassing four i.p. injections of MPTP–HCl in 1 day, 2 h apart (18 mg of free base per kg of body weight per injection). MPTP injections started 7 days after viral stereotaxic injections and mice were sacrificed 7 days after the MPTP injections. In both cases, control mice received an equivalent volume of 0.9% saline.

High-performance liquid chromatography

Following decapitation, the brain was carefully removed from the skull and the whole striatum was rapidly isolated on ice. After immediate weighing, the tissue was homogenized and deproteinized in 200 μl of 0.2 N perchloric acid solution (Merck KgaA, Darmstadt, Germany) containing 7.9 mM $Na_2S_2O_5$ and 1.3 mM Na_2EDTA (both by Riedel-de Haën AG, Seelze, Germany). The homogenate was centrifuged at 14 000 rpm for 30 min and the supernatant was stored at −80°C. Neurotransmitter analysis was performed by HPLC with an electrochemical detector (HPLC-ED), as described previously (56). Reverse-phase ion pair chromatography was used to assay in all sample DA and its metabolites DOPAC and HVA. The mobile phase consisted of an acetonitrile (Merck KgaA)–50 mM phosphate buffer (10.5:89.5), pH 3.0, containing 300 mg/l 5-octylsulfonic acid sodium salt (Merck KgaA) as the ion-pair reagent and 20 mg/l of Na_2EDTA (Riedel-de Haën AG). Reference standards were prepared in deproteinization buffer. The sensitivity of the assay was tested for each series of samples using external standards. Assays were performed on a BAS-LC4B HPLC system with an amperometric detector. The working electrode was glassy carbon; the columns were Thermo Hypersil-Keystone, 150 × 2.1 mm 5 μm Hypersil, Elite C18 (Thermo Electron, Cheshire, UK). The HPLC system was connected to a computer, which was used to quantify all compounds by comparison of the area under the peaks with the area of reference standards with specific HPLC software (Chromatography Station for Windows). The limit of detection was 1 pg/27 μl (injection volume).

Western blot analysis

For western immunoblotting analysis, animals were sacrificed by cervical dislocation; brains were harvested, dissected on ice to obtain the region of interest and immediately frozen. All animals were processed in a similar manner. Tissue was stored at −80°C until further use. rAd WT or S18Y UCH-L1 and rAd-EGFP-injected mice were sacrificed at 14 days post-injection. The ventral midbrain encompassing the substantia nigra and the striata from injected and uninjected hemispheres were then rapidly dissected and homogenized in Triton extraction buffer (150 mM NaCl, 50 mM Tris, pH 7.6, 1% Triton-X-100, 2 mM EDTA) containing protease inhibitors. The lysate was then centrifuged (14 000 g for 10 min) to collect the supernatant (''soluble fraction'). The pellet was incubated with lysis buffer supplemented with 0.1% SDS and centrifuged under the same conditions. The resulting supernatant represents the 'insoluble fraction' (SDS soluble). Western blot analysis on 50 μg protein was carried out with primary antibodies against FLAG (mouse immunoglobulin G (IgG), 1:1000; Anti-FLAG M2, Sigma), UCH-L1 (PGP 9.5) (rabbit IgG, 1:2000, Affinity), GFP (mouse IgG, 1:1000, Santa Cruz Biotechnology, CA, USA), TH (rabbit IgG, 1:2.000; Calbiochem, San Diego, CA, USA), DA transporter (DAT) (rat IgG, 1:1.500; Chemicon, Temecula, CA, USA) and β-actin antibody to confirm equal protein loading (mouse IgG, 1:10 000; Sigma). Detection and quantification were performed using the Gel analyzer Imaging System.

Immunohistological analysis and quantification

Tissue processing. For the phenotypic analysis of the dopaminergic system of *gad* mice or their corresponding littermates, animals were sacrificed at 14 days after the first MPTP injection. For the histological analysis of mice injected with the adenoviruses expressing WT or S18Y UCH-L1 or the control viruses EGFP or AdO, animals were sacrificed at 14 days post-adenoviral injection (7 days after MPTP injection). Mice were deeply anesthetized by an overdose of pentobarbital and perfused transcardially first with phosphate-buffered saline (PBS) and then with ice-cold 4% paraformaldehyde in 0.1 M phosphate buffer 1 (PBS; pH 7.2). Brains were quickly removed, post-fixed in the same fixative overnight at 4°C, cryoprotected in 15% sucrose (in 0.1 M PBS for 24 h) and in 30% sucrose (in 0.1 M PBS for 24 h) at 4°C, frozen, and stored at −80°C until sectioning. For each mouse, free-floating cryostat-cut sections (30 μm) were collected using a Bright cryostat at −25°C at the levels of striatum (AP, 0.2 mm from bregma) and the entire midbrain (AP, −5.6 mm from bregma) (57). As described previously (58), sections were first quenched for 10 min in 3% H_2O_2/10% methanol mixture and subsequently blocked with 10% normal goat serum [NGS; 1 h, room temperature (RT)]. The polyclonal anti-TH antibody (1:2.000; Calbiochem) was added for 48 h (4°C), followed by incubation with a biotinylated anti-rabbit antibody (1:1500; Vector Laboratories, Burlingame, CA, USA) in 1% NGS for 1 h and avidin–biotin peroxidase complex for 1 h in RT (ABC Elite; Vector Laboratories). Staining was visualized using diaminobenzidine (Sigma) as a chromogen (59). The specificity was tested in adjacent sections with the primary or the secondary antibody omitted. The sections were stained with cresyl violet (Nissl staining), and then dehydrated in graded ethanol and cover slipped.

Immunohistochemistry. Primary antibodies used in this study were TH (rabbit IgG, 1:2000, Calbiochem; mouse IgG, 1:1000, Chemicon), FLAG (mouse IgG, 1:1000; Anti-FLAG M2, Sigma), UCH-L1 (PGP 9.5) (rabbit IgG, 1:2000, Affinity) and GFP (mouse IgG, 1:1000, Santa Cruz Biotechnology). For double-fluorescence labeling, we used secondary antibodies conjugated to Cy2 and Cy3 (Jackson ImmunoResearch, Suffolk, UK). For bright-field microscopy, we used biotinylated goat anti-rabbit or anti-mouse secondary antibodies (1:200; Vector Laboratories).

Quantitative analysis of fluorescence. To assess the levels of UCH-L1 overexpression in the Flag-positive retrogradely transduced neurons, as well as the percentage of TH- and Flag-positive neurons of the SNpc of animals injected with the rAd-WT or rAd-S18Y-UCH-L1-Flag, we performed quantitative fluorescence analysis and cell counts using Image J software, as described previously (29). Results are presented as means ± SEM.

Stereological quantification of TH-positive and Nissl-stained neurons. Unbiased stereological estimation of the number of TH-positive and Nissl-stained neurons in SNpc was carried out according to the optical fractionator method using the

NewCast Module in VIS software (Visiopharm A/S, Horsholm, Denmark). Every fourth section throughout the entire extent of the SNpc was included in the counting procedure, which yielded a total of 10 sections containing substantia nigra (Franklin and Paxinos, 2001). All quantifications were done in a blinded fashion. The SNpc was delineated by using a ×4 objective and the actual counting was performed using a ×60 Plan-Apo oil objective (numerical aperture = 1.4) on a Nikon 80i microscope equipped with an *X*–*Y* motorized stage, a *Z*-axis motor and a high-precision linear encoder (Heidenhein). Coefficient of error attributable to the sampling was calculated according to Gundersen and Jensen (60) and values ≤0.10 were accepted.

Primary neuronal cultures

Cultures of rat (embryonic day 18, E18) cortical neurons were prepared as described previously (61,62). Cells were plated onto poly-D-lysine-coated dishes at a density of ∼150 000–200 000/cm^2 and maintained in Neurobasal medium, with B27 supplement (Invitrogen), L-glutamine (0.5 mM) and penicillin/streptomycin (1%). More than 98% of the cells cultured under these conditions represent post-mitotic neurons (63).

Immunocytochemistry

Cortical neurons grown on 24-well plates were fixed in freshly prepared 3.7% formaldehyde for 45 min. Blocking was with 10% NGS, 0.4% Triton X-100 for 1 h at RT. Mouse anti-M2 Flag (1:400; Sigma) antibody was applied overnight at 4°C; rAd-GFP virus was detected by direct immunofluorescence. The fluorescent mouse Cy3 secondary antibody (1:250, Jackson ImmunoResearch) was added for 1 h. The fluorescent marker Hoechst 33258 (1 μM; Sigma) was used to assess cell nuclei.

Assessment of MPP^+ toxicity

Neurons were cultured on poly-D-lysine-coated 24-well plates. Five days after plating, primary rat cortical cultures were transduced with 100 MOI of rAd viruses expressing WT or S18Y UCH-L1 or the control virus GFP. Two days later, these cultures were exposed to 40 μM MPP^+ and 24 h after MPP^+ addition, the medium was removed and cells were lysed in a detergent containing solution, which enables the quantification of viable cells by counting the number of intact nuclei in a haemacytometer (64,65). This method has been shown to be reproducible and accurate and to correlate well with other methods of assessing cell survival–death (66). Cell counts were performed in triplicate and are reported as mean ± SE. Axonal degeneration and loss of neuritic processes were also observed using phase contrast microscopy.

Statistical analysis

All data are expressed as mean ± SEM. Statistical significance of differences was evaluated either with two way ANOVA for comparisons between WT and *gad* mice treated with saline or MPTP or with one-way ANOVA followed by the Student–Newman–Keuls' test. In one case, in the HPLC experiments in Figure 8, Student's *t*-paired test was used for comparisons between the contralateral and the ipsilateral side of rAd-S18Y-injected mice. Probability values <5% were considered significant.

SUPPLEMENTARY MATERIAL

Supplementary Material is available at *HMG* online.

Conflict of Interest statement. None declared.

FUNDING

This work was supported by a Rapid Innovation Award from Michael J Fox Research Foundation to L.S., a FP7/REGPOT-2008-1 to LS, a PENED grant from the Hellenic General Secretariat of Research and Technology (grant to E.K. and L.S.) and by an EMBO Travel Fellowship to E.K., and by FIS-ISCIII grants to M.V. and C.P. D.S.P. was funded by the Canadian Institutes of Health Research.

REFERENCES

1. Wilkinson, K.D., Lee, K.M., Deshpande, S., Duerksen-Hughes, P., Boss, J.M. and Pohl, J. (1989) The neuron-specific protein PGP 9.5 is a ubiquitin carboxyl-terminal hydrolase. *Science*, **246**, 670–673.
2. Nijman, S.M., Luna-Vargas, M.P., Velds, A., Brummelkamp, T.R., Dirac, A.M., Sixma, T.K. and Bernards, R. (2005) A genomic and functional inventory of deubiquitinating enzymes. *Cell*, **123**, 773–786.
3. Setsuie, R. and Wada, K. (2007) The functions of UCH-L1 and its relation to neurodegenerative diseases. *Neurochem. Int.*, **51**, 105–111.
4. Saigoh, K., Wang, Y.L., Suh, J.G., Yamanishi, T., Sakai, Y., Kiyosawa, H., Harada, T., Ichihara, N., Wakana, S., Kikuchi, T. *et al.* (1999) Intragenic deletion in the gene encoding ubiquitin carboxy-terminal hydrolase in gad mice. *Nat. Genet.*, **23**, 47–51.
5. Chen, F., Sugiura, Y., Myers, K.G., Liu, Y. and Lin, W. (2010) Ubiquitin carboxyl-terminal hydrolase L1 is required for maintaining the structure and function of the neuromuscular junction. *Proc. Natl Acad. Sci. USA*, **107**, 1636–1641.
6. Gasser, T. (2009) Molecular pathogenesis of Parkinson disease: insights from genetic studies. *Expert Rev. Mol. Med.*, **11**, e22.
7. Leroy, E., Boyer, R., Auburger, G., Leube, B., Ulm, G., Mezey, E., Harta, G., Brownstein, M.J., Jonnalagada, S., Chernova, T. *et al.* (1998) The ubiquitin pathway in Parkinson's disease. *Nature*, **395**, 451–452.
8. Maraganore, D.M., Farrer, M.J., Hardy, J.A., Lincoln, S.J., McDonnell, S.K. and Rocca, W.A. (1999) Case-control study of the ubiquitin carboxy-terminal hydrolase L1 gene in Parkinson's disease. *Neurology*, **53**, 1858–1860.
9. Maraganore, D.M., Lesnick, T.G., Elbaz, A., Chartier-Harlin, M.C., Gasser, T., Kruger, R., Hattori, N., Mellick, G.D., Quattrone, A., Satoh, J. *et al.* (2004) UCHL1 is a Parkinson's disease susceptibility gene. *Ann. Neurol.*, **55**, 512–521.
10. Elbaz, A., Levecque, C., Clavel, J., Vidal, J.S., Richard, F., Correze, J.R., Delemotte, B., Amouyel, P., Alperovitch, A., Chartier-Harlin, M.C. *et al.* (2003) S18Y polymorphism in the UCH-L1 gene and Parkinson's disease: evidence for an age-dependent relationship. *Mov. Disord.*, **18**, 130–137.
11. Satoh, J. and Kuroda, Y. (2001) A polymorphic variation of serine to tyrosine at codon 18 in the ubiquitin C-terminal hydrolase-L1 gene is associated with a reduced risk of sporadic Parkinson's disease in a Japanese population. *J. Neurol. Sci.*, **189**, 113–117.
12. Carmine Belin, A., Westerlund, M., Bergman, O., Nissbrandt, H., Lind, C., Sydow, O. and Galter, D. (2007) S18Y in ubiquitin carboxy-terminal hydrolase L1 (UCH-L1) associated with decreased risk of Parkinson's disease in Sweden. *Parkinsonism Relat. Disord.*, **13**, 295–298.
13. Healy, D.G., Abou-Sleiman, P.M., Casas, J.P., Ahmadi, K.R., Lynch, T., Gandhi, S., Muqit, M.M., Foltynie, T., Barker, R., Bhatia, K.P. *et al.*

(2006) UCHL-1 is not a Parkinson's disease susceptibility gene. *Ann. Neurol.*, **59**, 627–633.
14. Wang, L., Guo, J.F., Nie, L.L., Luo, L., Zuo, X., Shen, L., Jiang, H., Yan, X.X., Xia, K., Pan, Q. *et al.* (2011) Case-control study of the UCH-L1 S18Y variant in sporadic Parkinson's disease in the Chinese population. *J. Clin. Neurosci.*, **18**, 541–544.
15. Wintermeyer, P., Kruger, R., Kuhn, W., Muller, T., Woitalla, D., Berg, D., Becker, G., Leroy, E., Polymeropoulos, M., Berger, K. *et al.* (2000) Mutation analysis and association studies of the UCHL1 gene in German Parkinson's disease patients. *Neuroreport*, **11**, 2079–2082.
16. Levecque, C., Destee, A., Mouroux, V., Becquet, E., Defebvre, L., Amouyel, P. and Chartier-Harlin, M.C. (2001) No genetic association of the ubiquitin carboxy-terminal hydrolase-L1 gene S18Y polymorphism with familial Parkinson's disease. *J. Neural. Transm.*, **108**, 979–984.
17. Lincoln, S., Vaughan, J., Wood, N., Baker, M., Adamson, J., Gwinn-Hardy, K., Lynch, T., Hardy, J. and Farrer, M. (1999) Low frequency of pathogenic mutations in the ubiquitin carboxy-terminal hydrolase gene in familial Parkinson's disease. *Neuroreport*, **10**, 427–429.
18. Mellick, G.D. and Silburn, P.A. (2000) The ubiquitin carboxy-terminal hydrolase-L1 gene S18Y polymorphism does not confer protection against idiopathic Parkinson's disease. *Neurosci. Lett.*, **293**, 127–130.
19. Savettieri, G., De Marco, E.V., Civitelli, D., Salemi, G., Nicoletti, G., Annesi, G., Ciro Candiano, I.C. and Quattrone, A. (2001) Lack of association between ubiquitin carboxy-terminal hydrolase L1 gene polymorphism and PD. *Neurology*, **57**, 560–561.
20. Zhang, Z.J., Burgunder, J.M., An, X.K., Wu, Y., Chen, W.J., Zhang, J.H., Wang, Y.C., Xu, Y.M., Gou, Y.R., Yuan, G.G. *et al.* (2008) Lack of evidence for association of a UCH-L1 S18Y polymorphism with Parkinson's disease in a Han-Chinese population. *Neurosci. Lett.*, **442**, 200–202.
21. Tan, E.K., Lu, C.S., Peng, R., Teo, Y.Y., Wu-Chou, Y.H., Chen, R.S., Weng, Y.H., Chen, C.M., Fung, H.C., Tan, L.C. *et al.* (2009) Analysis of the UCHL1 genetic variant in Parkinson's disease among Chinese. *Neurobiol. Aging*, **31**, 2194–2196.
22. Setsuie, R., Wang, Y.L., Mochizuki, H., Osaka, H., Hayakawa, H., Ichihara, N., Li, H., Furuta, A., Sano, Y., Sun, Y.J. *et al.* (2007) Dopaminergic neuronal loss in transgenic mice expressing the Parkinson's disease-associated UCH-L1 I93M mutant. *Neurochem. Int.*, **50**, 119–129.
23. Liu, Y., Fallon, L., Lashuel, H.A., Liu, Z. and Lansbury, P.T. Jr. (2002) The UCH-L1 gene encodes two opposing enzymatic activities that affect alpha-synuclein degradation and Parkinson's disease susceptibility. *Cell*, **111**, 209–218.
24. Choi, J., Levey, A.I., Weintraub, S.T., Rees, H.D., Gearing, M., Chin, L.S. and Li, L. (2004) Oxidative modifications and down-regulation of ubiquitin carboxyl-terminal hydrolase L1 associated with idiopathic Parkinson's and Alzheimer's diseases. *J. Biol. Chem.*, **279**, 13256–13264.
25. Butterfield, D.A., Gnjec, A., Poon, H.F., Castegna, A., Pierce, W.M., Klein, J.B. and Martins, R.N. (2006) Redox proteomics identification of oxidatively modified brain proteins in inherited Alzheimer's disease: an initial assessment. *J. Alzheimers Dis.*, **10**, 391–397.
26. Goto, A., Wang, Y.L., Kabuta, T., Setsuie, R., Osaka, H., Sawa, A., Ishiura, S. and Wada, K. (2009) Proteomic and histochemical analysis of proteins involved in the dying-back-type of axonal degeneration in the gracile axonal dystrophy (gad) mouse. *Neurochem. Int.*, **54**, 330–338.
27. Castegna, A., Thongboonkerd, V., Klein, J., Lynn, B.C., Wang, Y.L., Osaka, H., Wada, K. and Butterfield, D.A. (2004) Proteomic analysis of brain proteins in the gracile axonal dystrophy (gad) mouse, a syndrome that emanates from dysfunctional ubiquitin carboxyl-terminal hydrolase L-1, reveals oxidation of key proteins. *J. Neurochem.*, **88**, 1540–1546.
28. Nagamine, S., Kabuta, T., Furuta, A., Yamamoto, K., Takahashi, A. and Wada, K. (2010) Deficiency of ubiquitin carboxy-terminal hydrolase-L1 (UCH-L1) leads to vulnerability to lipid peroxidation. *Neurochem. Int.*, **57**, 102–110.
29. Kyratzi, E., Pavlaki, M. and Stefanis, L. (2008) The S18Y polymorphic variant of UCH-L1 confers an antioxidant function to neuronal cells. *Hum. Mol. Genet.*, **17**, 2160–2171.
30. Dauer, W. and Przedborski, S. (2003) Parkinson's disease: mechanisms and models. *Neuron*, **39**, 889–909.
31. Innamorato, N.G., Jazwa, A., Rojo, A.I., Garcia, C., Fernandez-Ruiz, J., Grochot-Przeczek, A., Stachurska, A., Jozkowicz, A., Dulak, J. and Cuadrado, A. (2010) Different susceptibility to the Parkinson's toxin MPTP in mice lacking the redox master regulator Nrf2 or its target gene heme oxygenase-1. *PLoS One*, **5**, e11838.
32. Zhou, H. and Beaudet, A.L. (2000) A new vector system with inducible E2a cell line for production of higher titer and safer adenoviral vectors. *Virology*, **275**, 348–357.
33. Kugler, S., Kilic, E. and Bahr, M. (2003) Human synapsin 1 gene promoter confers highly neuron-specific long-term transgene expression from an adenoviral vector in the adult rat brain depending on the transduced area. *Gene Ther.*, **10**, 337–347.
34. Smith, P.D., Crocker, S.J., Jackson-Lewis, V., Jordan-Sciutto, K.L., Hayley, S., Mount, M.P., O'Hare, M.J., Callaghan, S., Slack, R.S., Przedborski, S. *et al.* (2003) Cyclin-dependent kinase 5 is a mediator of dopaminergic neuron loss in a mouse model of Parkinson's disease. *Proc. Natl Acad. Sci. USA*, **100**, 13650–13655.
35. Crocker, S.J., Smith, P.D., Jackson-Lewis, V., Lamba, W.R., Hayley, S.P., Grimm, E., Callaghan, S.M., Slack, R.S., Melloni, E., Przedborski, S. *et al.* (2003) Inhibition of calpains prevents neuronal and behavioral deficits in an MPTP mouse model of Parkinson's disease. *J. Neurosci.*, **23**, 4081–4091.
36. Qu, D., Rashidian, J., Mount, M.P., Aleyasin, H., Parsanejad, M., Lira, A., Haque, E., Zhang, Y., Callaghan, S., Daigle, M. *et al.* (2007) Role of Cdk5-mediated phosphorylation of Prx2 in MPTP toxicity and Parkinson's disease. *Neuron*, **55**, 37–52.
37. Dusonchet, J., Kochubey, O., Stafa, K., Young, S.M. Jr, Zufferey, R., Moore, D.J., Schneider, B.L. and Aebischer, P. (2011) A rat model of progressive nigral neurodegeneration induced by the Parkinson's disease-associated G2019S mutation in LRRK2. *J. Neurosci.*, **31**, 907–912.
38. Przedborski, S. and Vila, M. (2003) The 1-methyl-4-phenyl-1,2,3,6-tetrahydropyridine mouse model: a tool to explore the pathogenesis of Parkinson's disease. *Ann. N. Y. Acad. Sci.*, **991**, 189–198.
39. Xiromerisiou, G., Kyratzi, E., Dardiotis, E., Bozi, M., Tsimourtou, V., Stamboulis, E., Ralli, S., Vassilatis, D., Gourbali, V., Kountra, P.M. *et al.* (2011) Lack of association of the UCHL-1 gene with Parkinson's disease in a Greek cohort: a haplotype-tagging approach. *Mov. Disord.* May 28. doi: 10.1002/mds.23694. [Epub ahead of print].
40. Bonifati, V., Rizzu, P., van Baren, M.J., Schaap, O., Breedveld, G.J., Krieger, E., Dekker, M.C., Squitieri, F., Ibanez, P., Joosse, M. *et al.* (2003) Mutations in the DJ-1 gene associated with autosomal recessive early-onset parkinsonism. *Science*, **299**, 256–259.
41. Hague, S., Rogaeva, E., Hernandez, D., Gulick, C., Singleton, A., Hanson, M., Johnson, J., Weiser, R., Gallardo, M., Ravina, B. *et al.* (2003) Early-onset Parkinson's disease caused by a compound heterozygous DJ-1 mutation. *Ann. Neurol.*, **54**, 271–274.
42. Hering, R., Strauss, K.M., Tao, X., Bauer, A., Woitalla, D., Mietz, E.M., Petrovic, S., Bauer, P., Schaible, W., Muller, T. *et al.* (2004) Novel homozygous p.E64D mutation in DJ1 in early onset Parkinson disease (PARK7). *Hum. Mutat.*, **24**, 321–329.
43. Martinat, C., Shendelman, S., Jonason, A., Leete, T., Beal, M.F., Yang, L., Floss, T. and Abeliovich, A. (2004) Sensitivity to oxidative stress in DJ-1-deficient dopamine neurons: an ES-derived cell model of primary Parkinsonism. *PLoS Biol.*, **2**, e327.
44. Simon-Sanchez, J., Schulte, C., Bras, J.M., Sharma, M., Gibbs, J.R., Berg, D., Paisan-Ruiz, C., Lichtner, P., Scholz, S.W., Hernandez, D.G. *et al.* (2009) Genome-wide association study reveals genetic risk underlying Parkinson's disease. *Nat. Genet.*, **41**, 1308–1312.
45. Simon-Sanchez, J. and Singleton, A. (2008) Genome-wide association studies in neurological disorders. *Lancet Neurol.*, **7**, 1067–1072.
46. Satake, W., Nakabayashi, Y., Mizuta, I., Hirota, Y., Ito, C., Kubo, M., Kawaguchi, T., Tsunoda, T., Watanabe, M., Takeda, A. *et al.* (2009) Genome-wide association study identifies common variants at four loci as genetic risk factors for Parkinson's disease. *Nat. Genet.*, **41**, 1303–1307.
47. Liu, Z., Meray, R.K., Grammatopoulos, T.N., Fredenburg, R.A., Cookson, M.R., Liu, Y., Logan, T. and Lansbury, P.T. Jr (2009) Membrane-associated farnesylated UCH-L1 promotes alpha-synuclein neurotoxicity and is a therapeutic target for Parkinson's disease. *Proc. Natl Acad. Sci. USA*, **106**, 4635–4640.
48. Yamazaki, K., Wakasugi, N., Tomita, T., Kikuchi, T., Mukoyama, M. and Ando, K. (1988) Gracile axonal dystrophy (GAD), a new neurological mutant in the mouse. *Proc. Soc. Exp. Biol. Med.*, **187**, 209–215.
49. Sakurai, M., Sekiguchi, M., Zushida, K., Yamada, K., Nagamine, S., Kabuta, T. and Wada, K. (2008) Reduction in memory in passive avoidance learning, exploratory behaviour and synaptic plasticity in mice

with a spontaneous deletion in the ubiquitin C-terminal hydrolase L1 gene. *Eur. J. Neurosci.*, **27**, 691–701.
50. Cartier, A.E., Djakovic, S.N., Salehi, A., Wilson, S.M., Masliah, E. and Patrick, G.N. (2009) Regulation of synaptic structure by ubiquitin C-terminal hydrolase L1. *J. Neurosci.*, **29**, 7857–7868.
51. Harada, T., Harada, C., Wang, Y.L., Osaka, H., Amanai, K., Tanaka, K., Takizawa, S., Setsuie, R., Sakurai, M., Sato, Y. *et al.* (2004) Role of ubiquitin carboxy terminal hydrolase-L1 in neural cell apoptosis induced by ischemic retinal injury in vivo. *Am. J. Pathol.*, **164**, 59–64.
52. Kwon, J., Wang, Y.L., Setsuie, R., Sekiguchi, S., Sato, Y., Sakurai, M., Noda, M., Aoki, S., Yoshikawa, Y. and Wada, K. (2004) Two closely related ubiquitin C-terminal hydrolase isozymes function as reciprocal modulators of germ cell apoptosis in cryptorchid testis. *Am. J. Pathol.*, **165**, 1367–1374.
53. Shen, H., Sikorska, M., Leblanc, J., Walker, P.R. and Liu, Q.Y. (2006) Oxidative stress regulated expression of ubiquitin carboxyl-terminal hydrolase-L1: role in cell survival. *Apoptosis*, **11**, 1049–1059.
54. He, T.C., Zhou, S., da Costa, L.T., Yu, J., Kinzler, K.W. and Vogelstein, B. (1998) A simplified system for generating recombinant adenoviruses. *Proc. Natl Acad. Sci. USA*, **95**, 2509–2514.
55. Jackson-Lewis, V. and Przedborski, S. (2007) Protocol for the MPTP mouse model of Parkinson's disease. *Nat. Protoc.*, **2**, 141–151.
56. Pitychoutis, P.M., Nakamura, K., Tsonis, P.A. and Papadopoulou-Daifoti, Z. (2009) Neurochemical and behavioral alterations in an inflammatory model of depression: sex differences exposed. *Neuroscience*, **159**, 1216–1232.
57. Franklin, K.B.J. and Paxinos, G. (2001) *The Mouse Brain in Stereotaxic Coordinates*, Academic press, San Diago.
58. Jackson-Lewis, V., Vila, M., Djaldetti, R., Guegan, C., Liberatore, G., Liu, J., O'Malley, K.L., Burke, R.E. and Przedborski, S. (2000) Developmental cell death in dopaminergic neurons of the substantia nigra of mice. *J. Comp. Neurol.*, **424**, 476–488.
59. Vila, M., Vukosavic, S., Jackson-Lewis, V., Neystat, M., Jakowec, M. and Przedborski, S. (2000) Alpha-synuclein up-regulation in substantia nigra dopaminergic neurons following administration of the parkinsonian toxin MPTP. *J. Neurochem.*, **74**, 721–729.
60. Gundersen, H.J. and Jensen, E.B. (1987) The efficiency of systematic sampling in stereology and its prediction. *J. Microsc.*, **147**, 229–263.
61. Vogiatzi, T., Xilouri, M., Vekrellis, K. and Stefanis, L. (2008) Wild type alpha-synuclein is degraded by chaperone-mediated autophagy and macroautophagy in neuronal cells. *J. Biol. Chem.*, **283**, 23542–23556.
62. Stefanis, L., Park, D.S., Friedman, W.J. and Greene, L.A. (1999) Caspase-dependent and -independent death of camptothecin-treated embryonic cortical neurons. *J. Neurosci.*, **19**, 6235–6247.
63. Rideout, H.J. and Stefanis, L. (2002) Proteasomal inhibition-induced inclusion formation and death in cortical neurons require transcription and ubiquitination. *Mol. Cell Neurosci.*, **21**, 223–238.
64. Farinelli, S.E., Greene, L.A. and Friedman, W.J. (1998) Neuroprotective actions of dipyridamole on cultured CNS neurons. *J. Neurosci.*, **18**, 5112–5123.
65. Rukenstein, A., Rydel, R.E. and Greene, L.A. (1991) Multiple agents rescue PC12 cells from serum-free cell death by translation- and transcription-independent mechanisms. *J. Neurosci.*, **11**, 2552–2563.
66. Stefanis, L., Troy, C.M., Qi, H. and Greene, L.A. (1997) Inhibitors of trypsin-like serine proteases inhibit processing of the caspase Nedd-2 and protect PC12 cells and sympathetic neurons from death evoked by withdrawal of trophic support. *J. Neurochem.*, **69**, 1425–1437.